

N O T I C E

THIS DOCUMENT HAS BEEN REPRODUCED FROM
MICROFICHE. ALTHOUGH IT IS RECOGNIZED THAT
CERTAIN PORTIONS ARE ILLEGIBLE, IT IS BEING RELEASED
IN THE INTEREST OF MAKING AVAILABLE AS MUCH
INFORMATION AS POSSIBLE

DOE/NASA/20485-7
NASA TM-81714

Laboratory Evaluation of a "Pilot Cell Battery Protection Systems" for Photovoltaic Applications

(NASA-TM-81714) LABORATORY EVALUATION OF A
PILOT CELL BATTERY PROTECTION SYSTEM FOR
PHOTOVOLTAIC APPLICATIONS (NASA) 14 p
HC A02/MF A01 CSCI 10C

N81-24536

Unclas
G3/44 42470

Robert L. Cataldo and Ralph D. Thomas
National Aeronautics and Space Administration
Lewis Research Center



Work performed for
U.S. DEPARTMENT OF ENERGY
Conservation and Solar Energy
Division of Solar Thermal Energy Systems

Prepared for
Sixteenth Intersociety Energy Conversion Engineering Conference
Atlanta, Georgia, August 9-14, 1981

Laboratory Evaluation of a "Pilot Cell Battery Protection System" for Photovoltaic Applications

Robert L. Cataldo and Ralph D. Thomas
National Aeronautics and Space Administration
Lewis Research Center
Cleveland, Ohio 44135

Work performed for
U.S. DEPARTMENT OF ENERGY
Conservation and Solar Energy
Division of Solar Thermal Energy Systems
Washington, D.C. 20545
Under Interagency Agreement DE-AI01-79ET20485

Prepared for
Sixteenth Intersociety Energy Conversion Engineering Conference
Atlanta, Georgia, August 9-14, 1981

LABORATORY EVALUATION OF A "PITOT CELL BATTERY PROTECTION SYSTEM" FOR PHOTOVOLTAIC APPLICATIONS

by Robert L. Cataldo and Ralph D. Thomas

National Aeronautics and Space Administration
Lewis Research Center
Cleveland, Ohio 44135

SUMMARY

The results of laboratory tests performed on a "Pilot Cell Battery Protection System," for use in photovoltaic power systems, shows this as a viable method of storage battery control. This method of limiting battery depth-of-discharge (DOD) has several advantages including: (1) temperature sensitivity, (2) rate sensitivity, and (3) state-of-charge (SOC) indication. The pilot cell concept is of particular interest for stand-alone photovoltaic power systems.

INTRODUCTION

The first photovoltaic village power system was installed at Schuchuli, Arizona on December 16, 1978 (ref. 1). The energy storage for the 3.5-kilowatt power system consists of 53 stationary type lead-acid cells connected in series. Special features of the lead-acid cells used in this application and manufactured by C&D Battery Division of Eltra Company, Plymouth Meeting, PA, are: two-fold glass fiber mat separators, microporous retainers, maintenance free lead-calcium alloy grids, extra electrolyte volume and cold climate, 1.300 specific gravity electrolyte. The cell capacity is 2380 ampere-hours at the 500 hour rate at 25° C. Therefore, the maximum energy storage of the main battery is 0.25 megawatt-hours.

The village energy storage battery is subjected to a seasonal deep discharge during the winter due to the reduced availability of solar insolation of this season. This causes a net deficit in the daily balance of charge ampere-hours available from the solar array to discharge ampere-hours of the assorted village loads. Without an adequate control system the battery could become totally discharged, and remain in this damaging condition for some months until the array output increases again in the spring.

The relationship between usable capacity and service life of a lead-calcium alloy battery after one or several sustained deep discharges (100 percent) is not fully understood. Therefore, a system that would both control and measure the main battery (DOD) was designed.

The system designed to protect the battery is called the Pilot Cell Battery Protection System (PCBPS). The system consists of four pilot cells that can be switched in and out of the main battery. The pilot cell capacities were selected to total 83 percent of the main battery capacity (based on nameplate capacities), thus limiting the main battery DOD to less than 83 percent.

The main battery is discharged in series with the number 1 pilot cell which has 44 percent of the main battery capacity. A voltage sensitive relay, measuring pilot cell voltage, removes the number 1 pilot cell when it is discharged and connects the number 2 (13 percent) pilot cell into the circuit. The system similarly steps down through the remaining 13 percent capacity pilot cells. When the last pilot cell is discharged all loads are removed from the system and the main battery is at about 80 percent DOD which is con-

sidered a safe depth to insure good charge acceptance upon recharge.

A test plan for laboratory evaluation of the system was designed to provide data about lead-calcium alloy batteries and the PCBPS. The objectives were to determine the validity of the PCBPS concept, to identify problem areas, and to evaluate three SOC indicators. These indicators were cell open circuit voltage, specific gravity, and ampere-hour integrator readings.

PROCEDURE

Table I shows the test plan used for evaluating the PCBPS. Phase I of the test plan consisted of life cycling one cell at the 2-hour rate (17.3 amp) to establish a nonabusive high rate discharge to be used in phase II. Phase II of the test plan was to validate the concept of the PCBPS, which is schematically represented in figure 1.

The cell used for phase I was a 2.0-volt, 50-ampere-hour (8 hr rate) (Exide Power Systems Division, ESB Incorporated, Philadelphia, PA) lead-calcium alloy, lead-acid with 1.220 sp. gr.

The cells used for phase II were C&D lead-calcium alloy lead-acid cells of the same type and construction, but with less capacity than the Schuchuli battery. The main battery was represented by one 2.0-volt, 219-ampere-hour cell. The number 1 pilot cell was 94 ampere-hours and the second, third, and fourth pilot cells each had 31 ampere-hour capacities at 25° C and at the 8-hour rate (table II).

Test equipment was specially designed and built to perform the phase II experiments (fig. 2). The charge control relay (CR5) was manually operated. Its function was to place the four pilot cells in parallel with respect to themselves and in series with the main cell for charging. Charging was accomplished by a constant voltage controlled power supply that allowed the charge current to taper off near the end of charge. Charging was terminated by cell voltage, which is limited by the set point selected on the meter relay (V5). Discharge is initiated by closing the discharge switch which operates discharge relay (CR1). The main and first pilot cell were discharged into a solid-state electronic load at constant current until the pilot cell voltage reached the cut off limit of 1.75 volts set on the voltage relay (V1). When the low limit was reached, CR1 dropped out removing pilot cell number 1 and CR6 picked up CR2 connecting pilot cell number 2 with the main cell. The main cell was discharged through pilot cells number 3 and then number 4 in similar manner.

The discharge currents used for the phase II tests reflected the load demand at Schuchuli. As each pilot cell is switched out, certain loads are taken off line according to a prioritized schedule. The current rates used in the test for each pilot cell were calculated from the "worst case" situation when all possible loads are drawing current from the battery only. Table II lists the current rates and cell plate areas for both Schuchuli and the test cells. The current densities for the test cells and Schuchuli pilot cells are iden-

tical. The calculated current rates were then increased by the factor 2-1/2 times, the safe limit determined in phase I.

When the 21 test cycles were completed, four additional discharges were performed to determine the actual SOC of the main cell following each pilot cell discharge. The main cell was discharged at the 8-hour rate (27.4 amp) to establish the remaining capacity. This test enabled the comparison of actual SOC of the main cell to the theoretical as estimated by the pilot cell capacities and discharge rates.

RESULTS

Phase I

The cell in phase I was cycled at the 2-hour discharge rate to 1.75 volts for 55 cycles. The cell received a 10-percent overcharge of the previous discharged ampere-hours to compensate for charging inefficiencies. The discharge capacity steadily decreased during the first four cycles (fig. 3) when the cell was charged at the recommended constant voltage of 2.45 volts. For the fifth cycle the charge method was changed to a constant current of 20 amperes, which stabilized the discharge capacity of the cell.

When lead-calcium alloy cells are charged with an insufficient current rate for gassing to occur, a vertical concentration gradient is established with the light acid at the top and heavy acid at the bottom of the cell. The gradient will be enhanced with cycling. The concentration gradient, called stratification, leads to non-uniform active material utilization and charging inefficiency, thereby causing a loss in available capacity (ref. 1). Therefore, the constant current charge method of 20 amperes was sufficient to gas the cell and eliminate the electrolyte stratification and thereby stabilize the discharge capacity.

The high rate discharge test demonstrated that a lead-calcium alloy lead-acid cell could achieve 55 deep cycles without incurring obvious physical damage. Therefore, this high rate was selected as a safe upper limit for the accelerated rates employed in phase II.

Phase II

During the phase II cycles, the scaled down version of the Schuchuli main battery and pilot cells were cycled under meter relay voltage control at accelerated rates discussed previously. The object was to verify the validity of the PCBPS, identify possible problem areas, evaluate and compare three different SOC indicators, and give some insight as to the life expectancy of the pilot cells.

Phase II data (fig. 4) shows charge voltage and charge and discharge ampere-hours for the main and pilot cells through 21 cycles. At the onset of the testing, a charge voltage was being sought that would charge the cells in a 24-hour period (cycles 1 to 6). However, it was then decided that the charging method should be similar to that at Schuchuli, with a maximum voltage limit of 2.42 volts per cell (cycles 7 to 20). As shown in figure 4, shortly after the charge voltage was changed, both the charge and discharge ampere-hours decreased. This decrease was expected as indicated by the phase I results. The electrolyte stratification steadily increased with cycling; particularly in the main and number 1 pilot cells, which contributed to the decrease in capacity. Figure 5, a plot of specific gravity at the top and bottom of the discharged number 1 pilot cell, shows the buildup of electrolyte stratification with continued cycling at the specified lower charge voltage. Again, as in the phase I studies, stratification was found to be associated with capacity

decreases. In addition to poor active material utilization, the lower portion of the plates softens in the higher concentration acid, whereby the active material dislodges from the grid, causing permanent loss of capacity. Thus, a charge voltage necessary to cause sufficient gassing to mix the electrolyte must be used or eventually a permanent loss in capacity will result.

Several methods can be employed to eliminate undesirable stratification. First, electrical electrolyte mixing can be used where sufficient voltage and current is available to gas and stir the electrolyte, as indicated in figure 5 during the fifth and sixth cycle. Figure 6 is a plot of charge voltage versus stratification under cyclic conditions. The first method, which is the most desirable, uses a charge voltage of 2.55 volts at room ambient temperature. This method reduces the amount of stratification with a minimum of gassing and plate erosion. Secondly, a period of several weeks will allow the concentration gradient to diffuse as shown in figure 5 (cycle number 21) where the charge time was 3 weeks at 2.42 volts. However, this method is highly impractical in cyclic operations of the battery. Third, a mechanical air lift pump can be used to stir the electrolyte; however, additional maintenance and costs will occur with this method.

Three battery SOC indicators, charge/discharge ampere-hour balance, open circuit cell voltage, and electrolyte specific gravity measurements were evaluated. The accuracies of the three SOC indicators are dependent on many factors, that is, cell age, SOC, and electrolyte stratification.

Ampere-Hour Integrator Method

When using an ampere-hour integrator, the ampere-hours measured on recharge can indicate a higher than actual state-of-charge (SOC) because of charging (coulombic) inefficiency. A portion of the charge current goes into gassing and this portion increases when higher charge rates are used, and as the cell becomes more fully charged. Therefore, the ampere-hour balance (charge AH/discharge AH) must be adjusted to compute the actual SOC. The factor used for this adjustment will change depending upon the operating point of the battery throughout the yearly cyclic rundown and recharge of the battery.

Open Circuit Voltage Method

Open circuit voltage measurements can be used to estimate the SOC of a lead-acid battery because voltage decreases linearly with decreasing SOC. It is necessary that the cell voltage be at equilibrium for maximum accuracy. The cell voltage deviates from equilibrium whenever it is being charged or discharged, and the amount of deviation is a function of current rate. As either charge or discharge rates are increased so is the amount of deviation. The time necessary for open circuit voltage to reach equilibrium after discharge current flow is on the order of several hours. However, this time is much longer following charge current flow as shown in figure 7. In many applications it is impractical to shut down the system to take open circuit voltage readings to accurately determine battery SOC.

Specific Gravity Method

Specific gravity readings from a hydrometer can yield accurate measurements of SOC. However, the specific gravity measured at the top of the cell can give a much lower reading if the electrolyte is stratified. This problem is of particular concern in tall lead-calcium grid cells where the electrolyte concentration

gradient has not had time to diffuse and reach equilibrium after a charge. Many of these large cells have electrolyte withdrawal tubes one third of the way down from the top of the cell, which gives an average reading of a stratified cell.

The results of determinations of the main cell SOC after each pilot cell discharge is shown in table III. The capacity remaining in the main cell was determined by discharging at the 8-hour rate, which is 27.4 amperes. This capacity is a measure of the actual SOC after the main cell has been discharged via each pilot cell. These values differ because the total capacity discharged from the main cell was greater than the 219 ampere-hour name plate 8-hour capacity. Adjusting for the increased main cell capacity would bring the actual and theoretical values into better correlation.

Appendix A contains a series of general load voltage discharge curves, recorded during cycle number 7, for the main and pilot cells.

CONCLUSION

The test results have indicated that the Pilot Cell Battery Protection System is a viable means of battery protection in photovoltaic systems. This method is of particular interest in remote stand-alone photovoltaic systems. The battery can be protected from damaging overdischarge by using the proper ratio of

pilot cell capacities to main battery capacity. A main battery (DOD) of 80 percent is desired. 80 Percent DOD allows maximum utility of the battery while assuring good rechargeability.

However, charge control and charge voltage is of particular concern with this technique since low charging voltages result in acid stratification which can lead to capacity loss and permanent damage to the cell plates. Therefore, if the normal operating charge voltage is too low, periodic voltage boost would help reduce acid stratification and prolong the operational life of the battery.

REFERENCES

1. Bifano, W. J., Ratajezak, A. F., and Ice, W. J., "Design and Fabrication of a Photovoltaic Power System for the Papago Indian Village of Schuchuli (Gunsight), Arizona," Twelfth Photovoltaic Specialists Conference, Conference Record, Institute of Electrical and Electronics Engineers, Inc., New York, 1978, pp. 1261-1267.

2. Sunn, Won G. Y., and Burrows, B. W., "Acid Stratification and Charge Characteristics of Low-Maintenance Industrial Cells," Presented at the Twelfth International Power Sources Symposium, Brighton, England, Sept. 1980, paper 39.

TABLE I. - OVERALL TEST PLAN FOR THE PILOT CELL BATTERY

PROTECTION SYSTEM EVALUATION

Test phase	Purpose	Test method	Measurements and calculations
I. Measure Pb-Ca cell capacity degeneration as a function of cell discharge rates. (Exide cells)	<ul style="list-style-type: none"> o To establish maximum discharge rate limits for phase II tests. 	<ul style="list-style-type: none"> o Charge/discharge cycling of single cells at high discharge rates. 	<ul style="list-style-type: none"> o Cell voltage o Cell current o Specific gravity o Ampere-hours in and out o Cycle number o Cycle interval duration o Cell state-of-charge as function of cycle number o State-of-charge comparisons
II. Life cycle a scaled-down version of the Schuchuli main battery and pilot cell load control circuit configuration at accelerated rates. (C&D cells)	<ul style="list-style-type: none"> o To verify the validity of the PCBPS prior to implementation at Schuchuli o To compare three separate rate indicators of state-of-charge for Pb-Ca cells. o Gain some insight on the life expectancy of pilot cells. 	<ul style="list-style-type: none"> o Meter-relay voltage controlled cycling of a capacity scaled-down version of the Schuchuli battery and pilot cell load control circuit, at accelerated discharge and cycling rates. 	<ul style="list-style-type: none"> o Basically the same as for phase I tests.

NOTE: Tests conducted at room temperature.

TABLE II. - CELL PLATE AREAS AND CURRENT RATES OF
SCHUCHULI AND TEST CELLS

	Pilot cells	Plate area (cm ²)	Current, amp
Schuchuli cells	1	8993	37.6
	2	3417	34.2
	3	3417	24.4
	4	3417	8.9
Test cells	1	1281	13.5
	2	427	10.75
	3	427	7.5
	4	427	2.75

TABLE III. - RESULTS OF THE REMAINING MAIN CELL CAPACITY
FOLLOWING PILOT CELL DISCHARGES

Run number	Pilot cell capacity, amp-hr				Main cell remaining capacity, amp-hr	Total main cell capacity, amp-hr
	Number 1	Number 2	Number 3	Number 4		
1	98.0	----	----	----	161.0	259.0
2	98.0	24.0	----	----	186.0	308.0
3	104.0	22.0	32.0	----	154.0	312.0
4	102.0	23.0	31.0	52.0	119.0	327.0

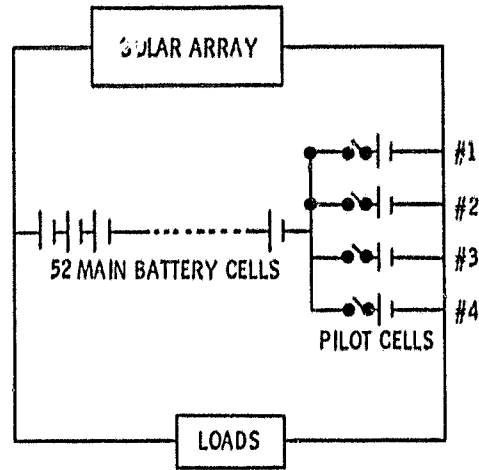


Figure 1. - Schematic representation of the pilot cell battery protection system.

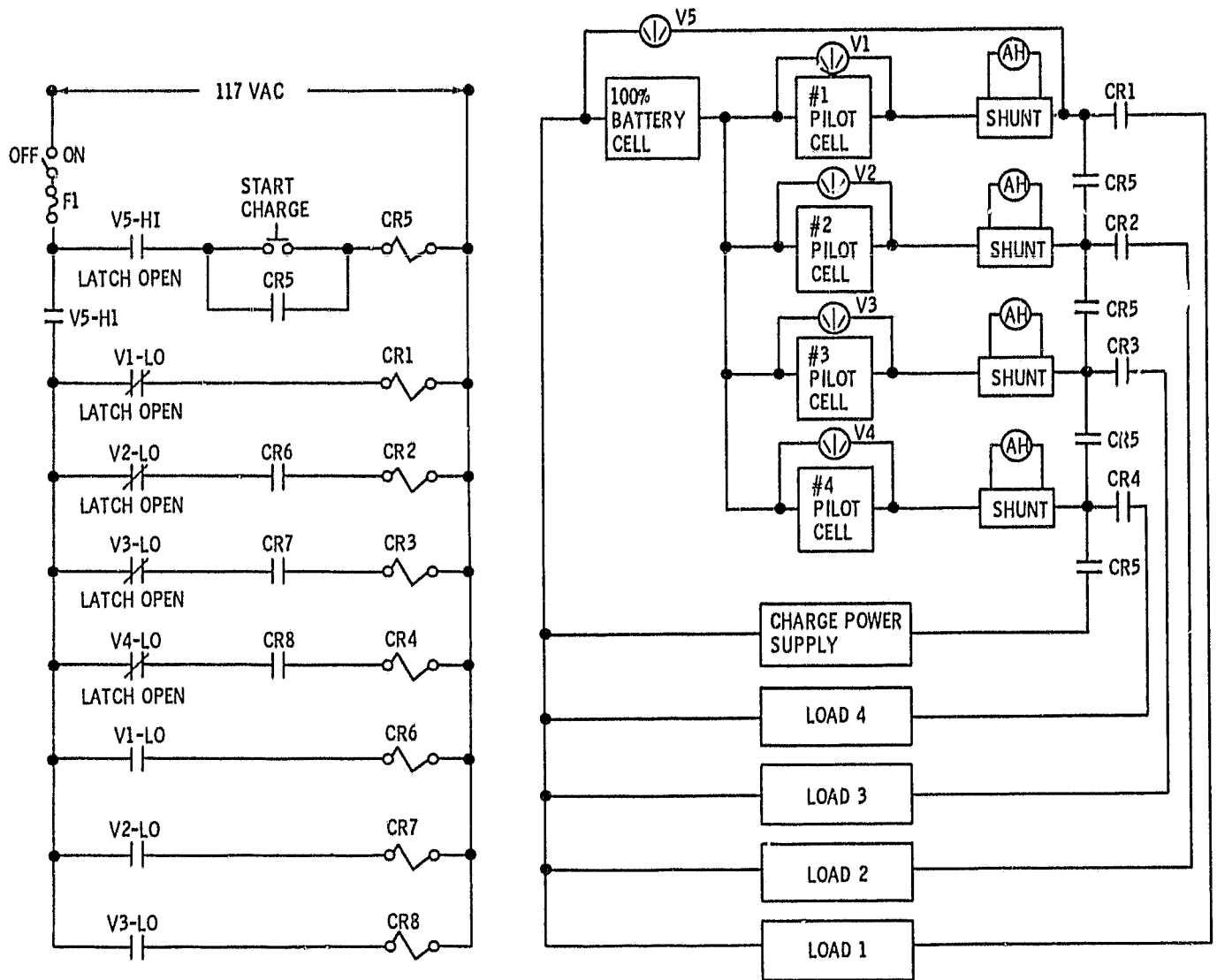


Figure 2. - Block diagram of the pilot cell test equipment.

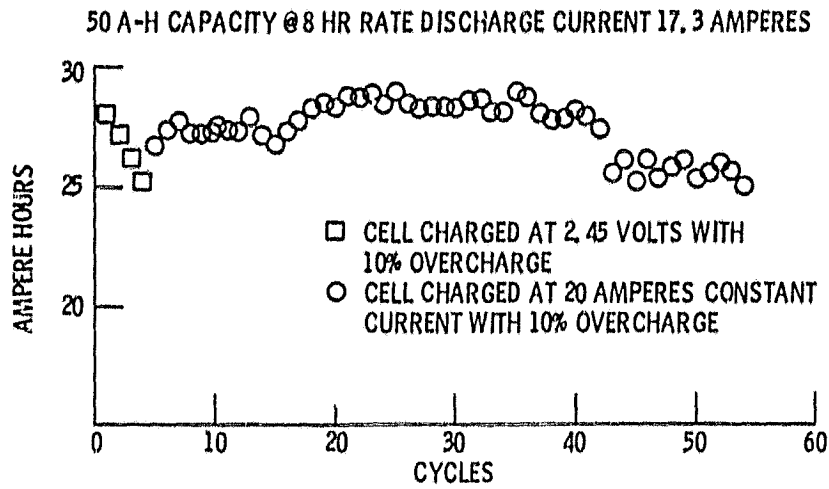


Figure 3. - High rate discharge capacity, VS cycles.

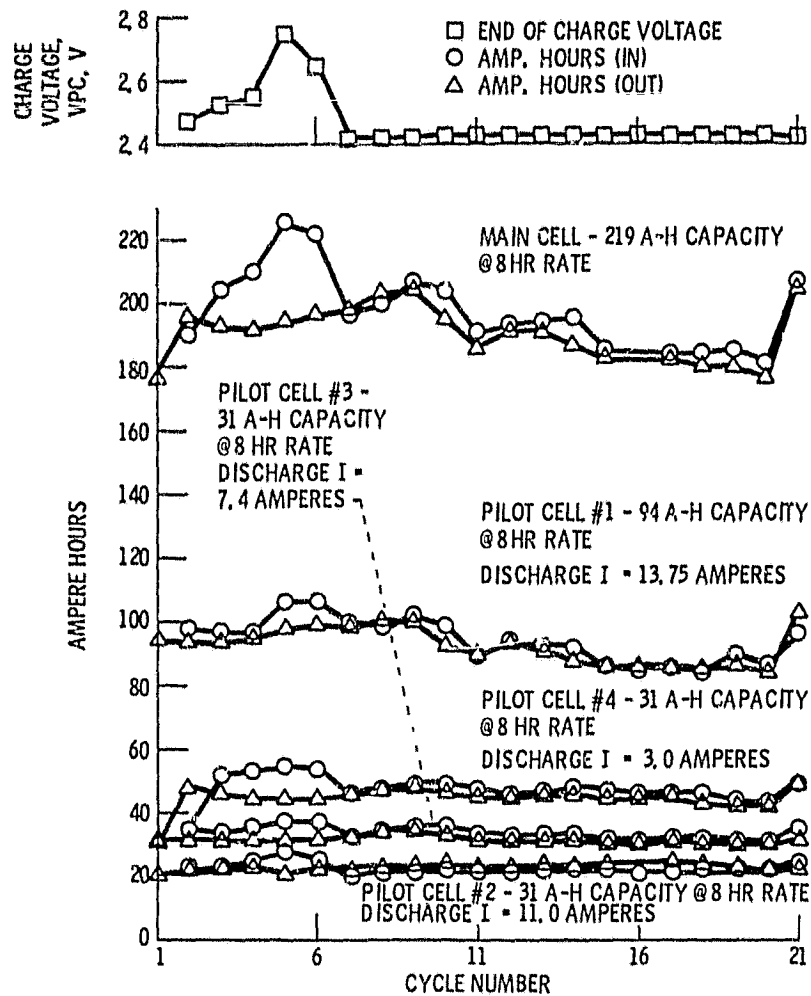


Figure 4. - Charge voltage, charge ampere-hours, discharge ampere-hours vs. cycle number.

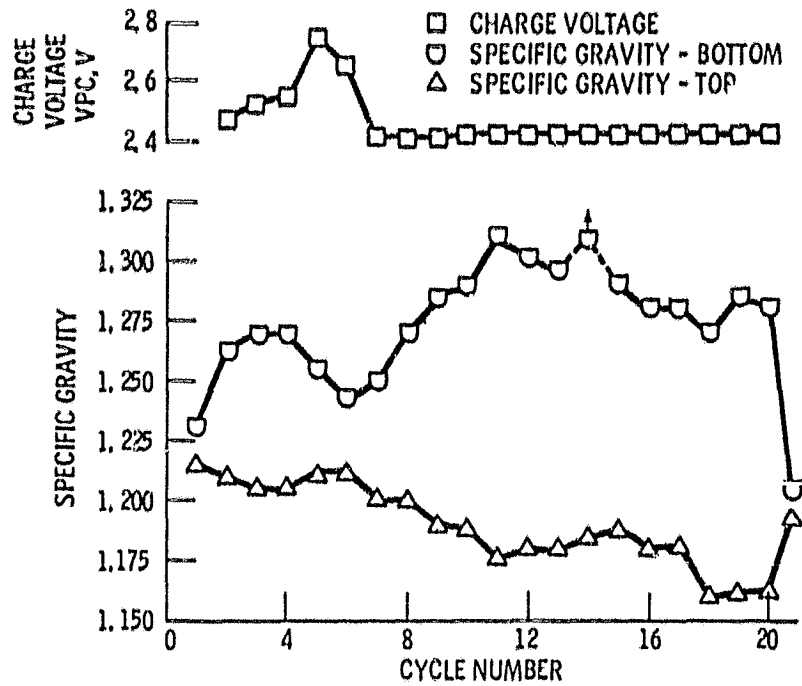


Figure 5. - Electrolyte stratification measured at the end of discharge for pilot cell #1.

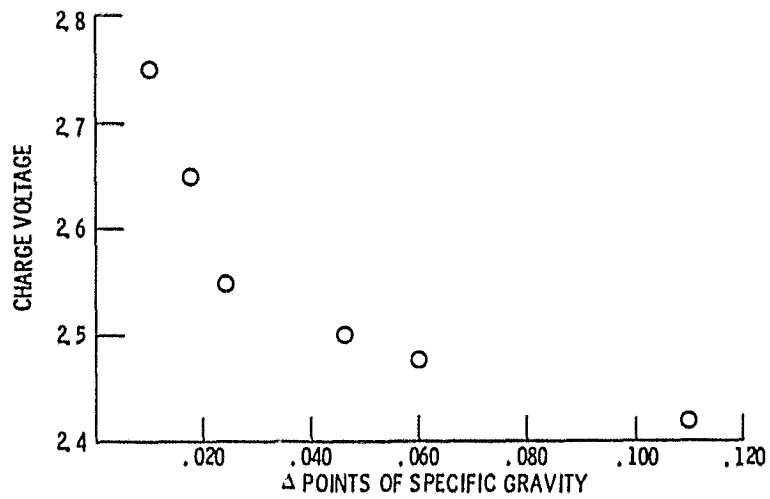


Figure 6. - Charge voltage vs. electrolyte stratification of a lead-calcium alloy cell under cyclic operation.

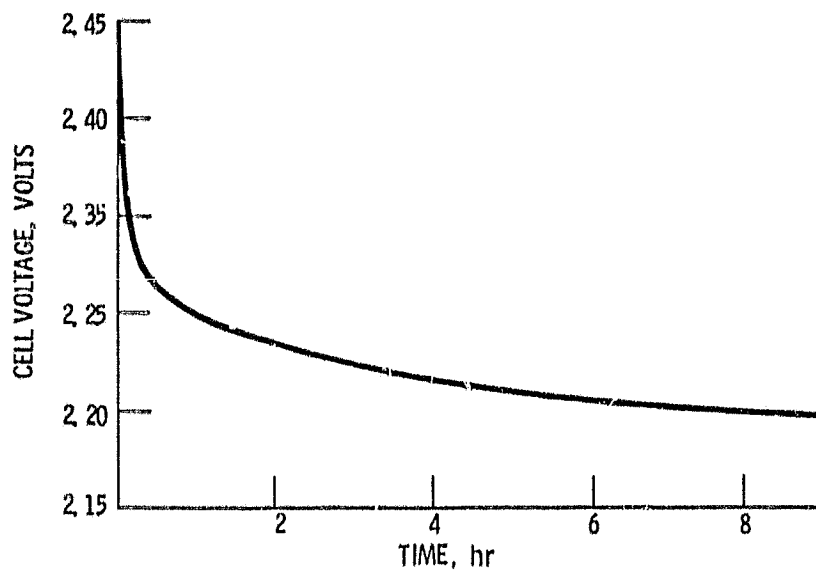


Figure 7. - Open circuit voltage decay vs. time, 77° F.

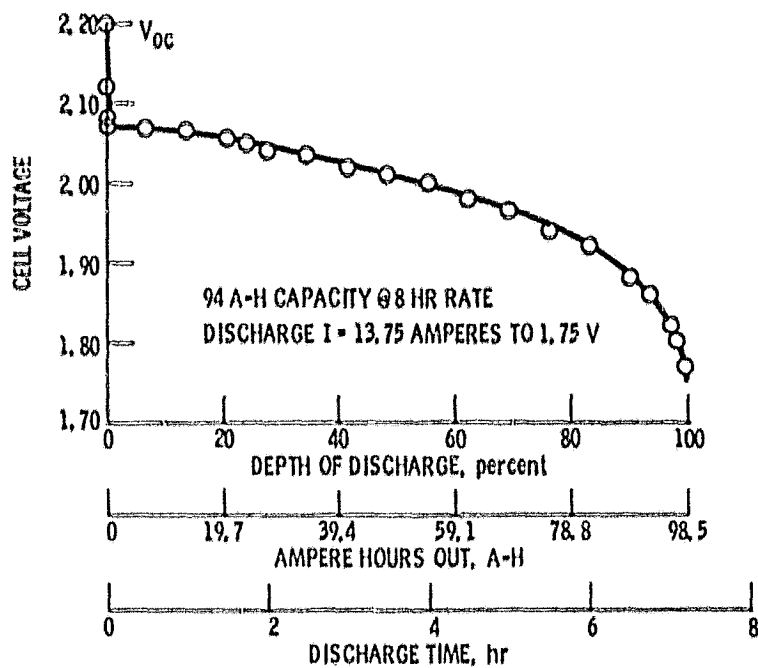


Figure A1, - Pilot cell #1, load voltage vs. discharge ampere-hours, depth-of-discharge and time.

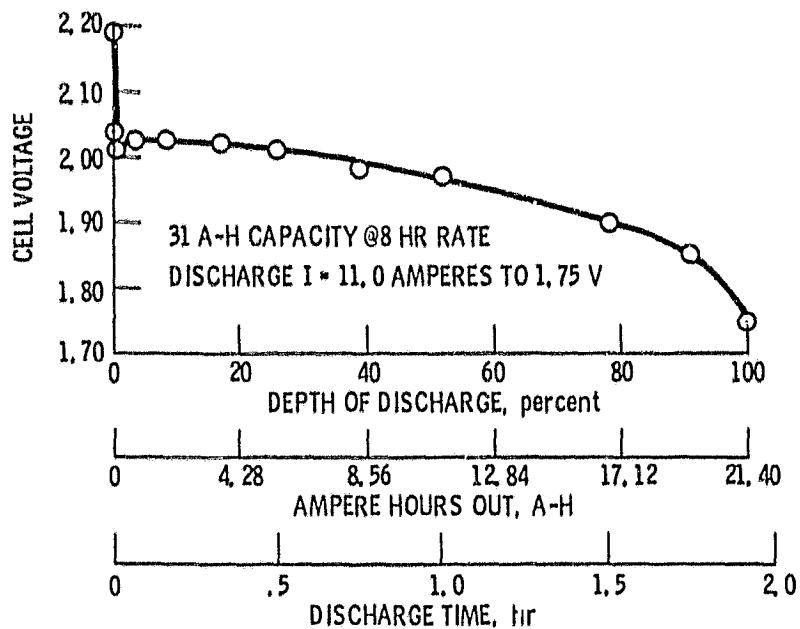


Figure A2, - Pilot cell #2, load voltage vs. discharge ampere-hours, depth-of-discharge and time.

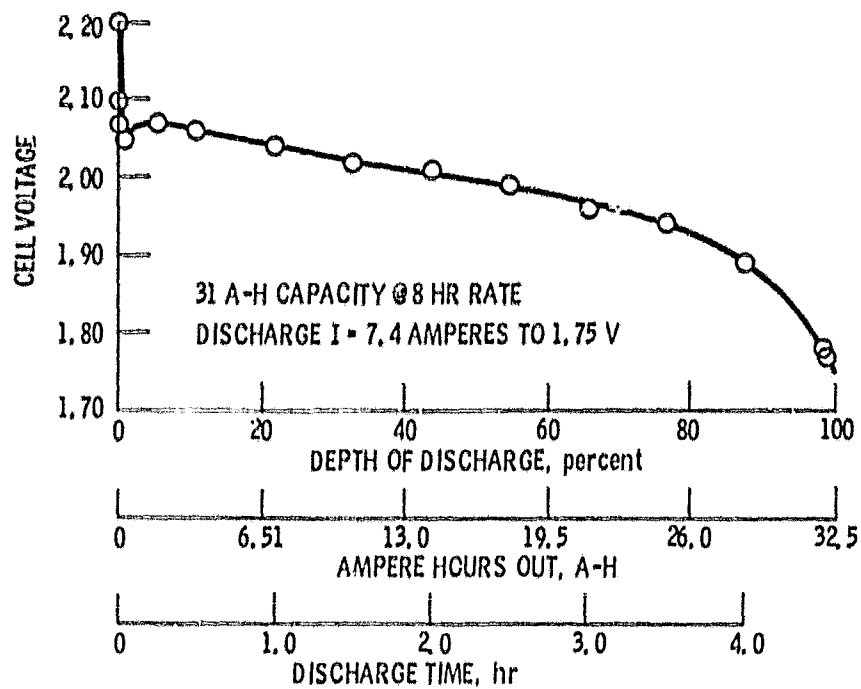


Figure A3. - Pilot cell #3, load voltage vs. discharge ampere-hours, depth-of-discharge and time.

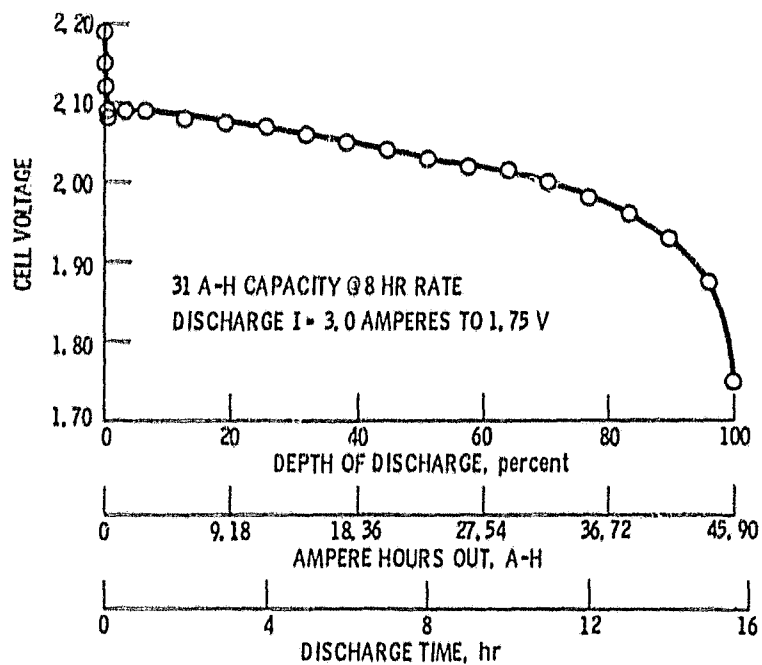


Figure A4. - Pilot cell #4, load voltage vs. discharge ampere-hours, depth-of-discharge and time.

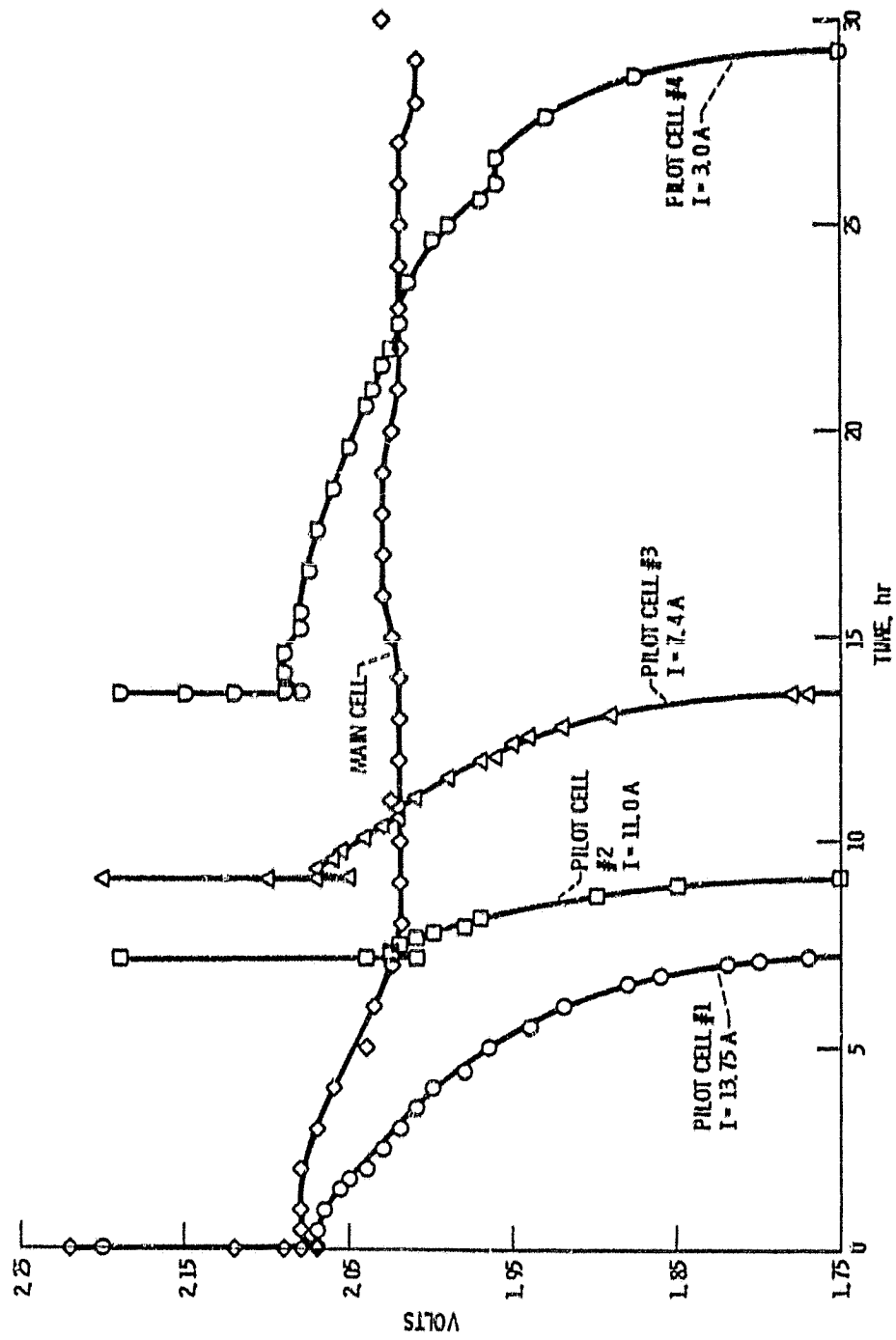


Figure A5. - Main cell discharge voltage profile compared to pilot cell discharge voltages profiles.